Reconstructing 3D subsurface salt flow

Stefan Back[1], Sebastian Amberg[1,2], Victoria Sachse[2,3], and Ralf Littke[2]

[1] Geological Institute, EMR, RWTH Aachen University, Germany
5 [2] Institute of Geology and Geochemistry of Petroleum and Coal, EMR, RWTH Aachen University, Germany
[3] Forschungszentrum Jülich GmbH, Projektträger Jülich, Germany

Correspondence to: Stefan Back (stefan.back@emr.rwth-aachen.de)

Abstract. Archimedes' principle states that the upward buoyant force exerted on a solid immersed in a fluid is equal to the

10   weight of the fluid that the solid displaces. In this 3D salt-reconstruction study we treat Zechstein evaporites in the subsurface

of the Netherlands, Central Europe, as a pseudo-fluid with a density of 2.2 g/cm^3, overlain by a lighter and solid overburden.

3D sequential removal (backstripping) of a differential sediment load above the Zechstein evaporites is used to incrementally

restore the top Zechstein surface. Assumption of a constant subsurface evaporite volume enables the stepwise reconstruction

of base Zechstein and the approximation of 3D salt-thickness change and lateral salt re-distribution over time.

15   The salt restoration presented is sensitive to any overburden thickness change irrespective if caused by tectonics,

basin tilt or sedimentary process. Sequential analysis of lateral subsurface salt loss and gain through time based on Zechstein

isopach difference maps provides new basin-scale insights into 3D subsurface salt flow and redistribution, supra-salt

depocentre development, the rise and fall of salt structures, and external forces' impact on subsurface salt movement. The 3D

reconstruction procedure described can serve as a template for analyzing other salt basins worldwide and provides a stepping

20   stone to physically sound fluid-dynamic models of salt tectonic provinces.

1 Introduction

Archimedes (c. 246 BC) proposed - in short - that the upward buoyant force exerted on a solid body immersed in a

fluid, whether fully or partially submerged, is equal to the weight of the fluid that the solid body displaces. This principle is an

25   essential law of physics and fluid mechanics. In geoscience, it forms e.g. the foundation of Airy Isostasy (Airy, 1855). This

study uses Archimedes' principle to reconstruct 3D subsurface salt flow through geological time by treating salt as a dense

fluid phase (ρ = 2.2 g/cm^3) in which lighter overburden rocks (solids) float (Fig. 1).
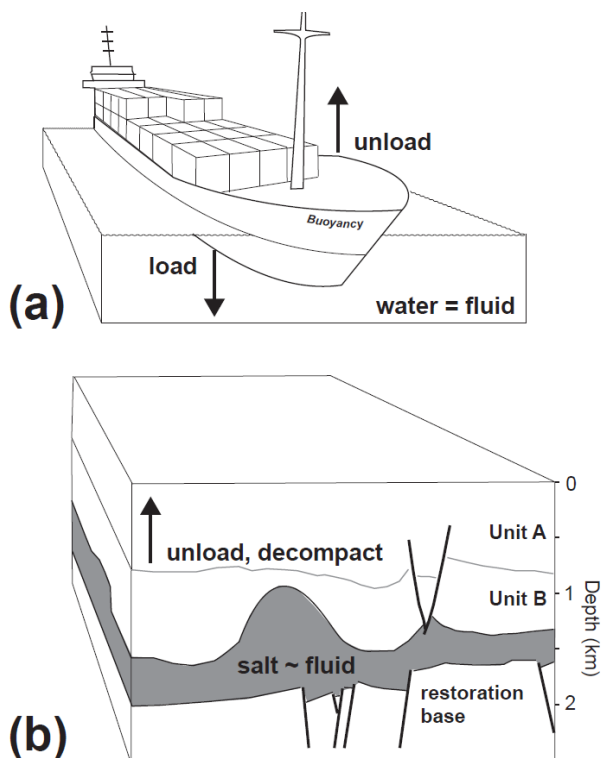
Figure 1. Cartoon of Archimedes' principle: (a) Ship loaded and unloaded floating on water. (b) Subsurface evaporites treated in analogy as
30   dense pseudo-fluid (ρ = 2.2 g/cm3) loaded by overburden rocks (solid). Backstripping of this study corresponds to unloading of the
overburden.

The buoyancy driver for subsurface salt movement was already proposed over 100 years ago by Aarhenius and

Lachmann (1912) and subsequently formalised by Barton (1933) and Nettleton (1934). Trusheim (1957, 1960) was a major

35   proponent of this theory, and applied this approach of analyzing salt flow to the NW European salt basin. In an early study on

potential nuclear-waste storage sites, Kehle (1980) specified that "sediment loading, not buoyancy, sensu stricto", drives

subsurface salt movement. Kehle (1988) pointed out several weaknesses in the original buoyancy theory mainly from a

hydrodynamic perspective. He emphasized two main controls for salt flow, gravity head and pressure head, and stressed the

importance of differential loading (resulting in high fluid-head gradients) for subsurface salt movement. Waltham (1997)

40   quantitatively investigated non-buoyant causes of salt movement (compression causing overburden thickening; flexural

overburden buckling; drag) and compared their effectiveness to buoyancy.

Few rocks behave as close as a Newtonian fluid as rock salt (e.g. Van Keken et al., 1993; Koyi, 2001; Gemmer et al., 2004; Jackson and Hudec, 2017). Davison et al. (1996) estimated the ratio between sedimentary-rock and evaporite-rock viscosity ranging from 50 to 10000. Thus, salt, similar to any fluid, cannot support shear stress (Hudec and Jackson, 2007; Warren, 2016). Various modelling studies have consequently treated subsurface salt as a pseudo-fluid flowing in the subsurface and consider its sedimentary overburden as solid (e.g. Jackson and Vendeville, 1994). This approach is supported by the observation that salt flows when loaded; and that faulting rather than folding characterizes deformation in the overburden (Davison 2009; Warren, 2016).

In this 3D backstripping study we avoid the complications of fluid-dynamic modelling of subsurface salt in that we simply measure 3D change in space through time rather than simulating details of a salt-flow regime. A governing assumption is that the studied overburden-salt system was in equilibrium throughout its history; i.e. that an isostatic relationship between the overburden and the salt substratum was maintained during crustal change induced by tectonics, differential sedimentation and/or erosion. Elementary backstripping theory proved sufficient to determine areas of accommodation loss and gain through time by overburden restoration, no matter what the exact flow properties of salt or the cause for loss and gain of depositional space. The backstripping and buoyancy compensation results presented are valid with the provision that salt flows into surplus space if available; and that subsurface evaporites will laterally move and redistribute when differentially loaded and the state of stress exceeding the limiting yield point (Kehle 1988). 1D, 2D, and 3D unloading and isostatic balancing algorithms that can be used to comprehend the reconstruction presented are readily available in several geological interpretation and modelling software.

2 Study area, data and methods

The Late Permian Zechstein Group in the subsurface of the onshore Netherlands, Central Europe (Fig. 2) comprises five evaporite cycles (Z1-Z5; Van Adrichem Boogaert and Kouwe, 1993; Geluk, 2007) with several hundreds of metres of rock salt and anhydrite deposited mainly in Z2 and Z3. The Zechstein Group is overlain by the Lower and Upper Germanic Trias groups (RB, RN), the Early and Middle Jurassic Altena Group (AT), the Late Jurassic Schieland-Scruff-Niedersachsen groups (SL, SG, SK), the Early Cretaceous Rijnland Group (KN), the Late Cretaceous Chalk Group (CK), the Paleogene

Lower (NL) and Middle (MN) North Sea groups and the Neogene to recent Upper North Sea Group (NU; Figs. 2b; 3a, b; TNO-NITG, 2004; Duin et al., 2006; Wong et al., 2007). For simplicity, this study treats the entire Permian Zechstein Group as one evaporite unit reacting to loading and unloading over geological time as a Newtonian fluid.
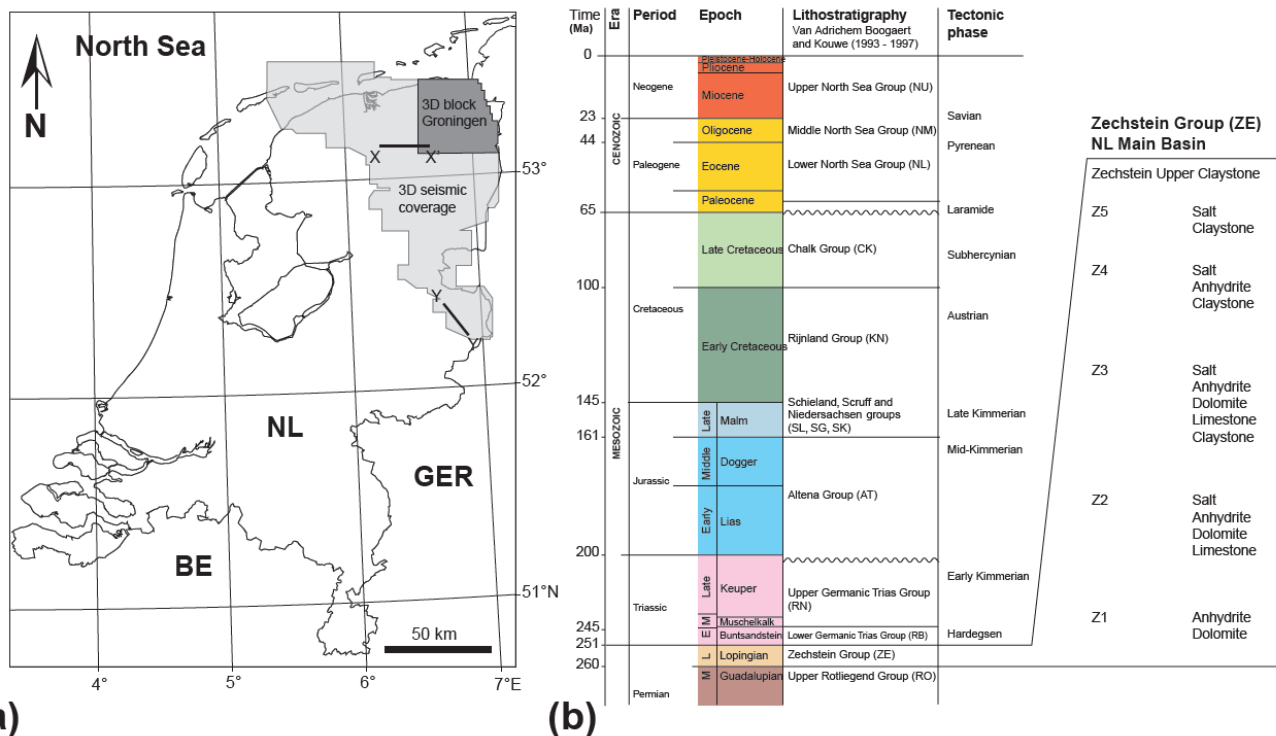
Figure 2. (a) Study area in the NE of the Netherlands and 3D seismic coverage. 3D block Groningen used for quality control. Lines X-X' and Y-Y' shown on Figure 3. BE = Belgium; GER = Germany; NL = The Netherlands. (b) Stratigraphy of the study area (after Van Adrichem Boogaert and Kouwe, 1993). Detailed lithostratigraphic subdivision of the Zechstein Group on the right. Stratigraphic abbreviations used on following figures.

Seven 3D surfaces in depth (m) from the public 3D geological model of the Netherlands "DGM-deep v5" form the study's stratigraphic framework. Horizon and lithology data are from the NLOG and DINOLoket public databases. Fifteen individual 3D seismic-reflection volumes were used for the identification of key structural elements, subsurface salt occurrence, unconformities and overburden stratigraphy (Fig. 2). Conversion of subsurface data from time (ms TWT) to depth (m) and vice versa was based on the velocity model of Van Dalfsen et al. (2006).
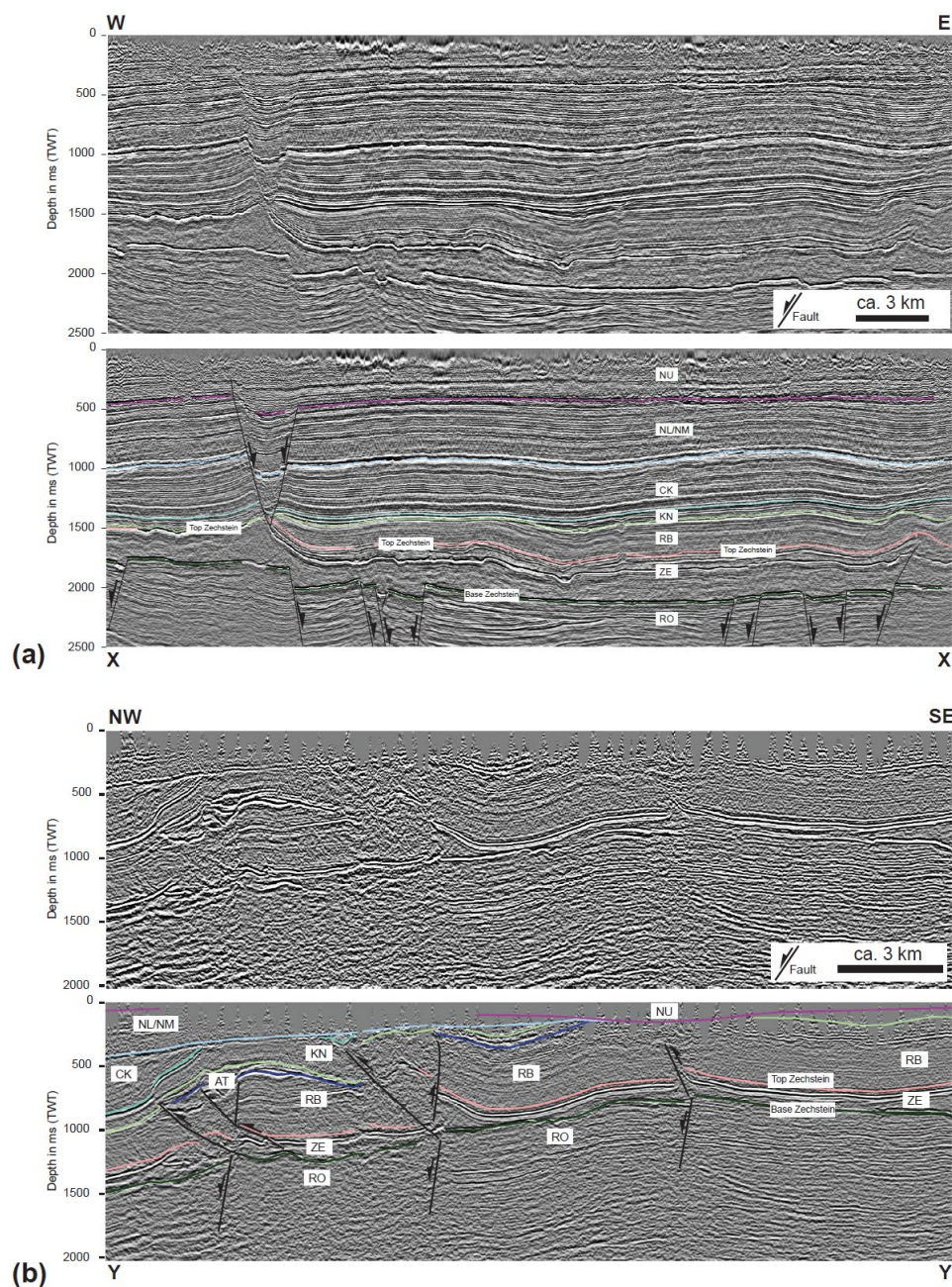
Figure 3. (a) Seismic-reflection line X-X' across the northern-central study area. Top – uninterpreted, base – interpreted. Note Zechstein unit (ZE) and bright, strong amplitude reflection near top imaging partly deformed and folded intra-salt Zechstein 3 stringer (Strozyk et al., 2012). (b) Seismic-reflection line Y-Y' across southern study area. Top – uninterpreted, base – interpreted. Note lack of upper Mesozoic and

85 Cenozoic Zechstein overburden in the south. For line locations and stratigraphic abbreviations see Figure 2.

Backstripping for stratigraphic restoration and salt-flow monitoring was initially applied to individual 3D seismic-reflection volumes (a.o. the 3D block Groningen; Fig. 2a). The method proved simple, quick and effective and was therefore immediately extended to the entire (ca. 10,000 km^2) NE Netherlands. Strata above the Zechstein were assigned average lithologies (Table 1) with a compaction trend sensu Sclater and Christie (1980). In all cases the present-day cumulative average density of the column of vertical overburden was lighter than the evaporate substratum (fluid with $\rho = 2.2$ g/cm^3) and should have been so in the past. Once a stratal cover unit was removed, the overburden response down to top Zechstein was to readjust due to buoyancy. In restoration scenario 1, buoyancy compensation was local ("Airy isostasy" above salt), i.e. only vertically below the load. Decompaction was omitted from backstripping to produce the simplest reconstruction. In restoration scenario 2, buoyancy compensation was kept local ("Airy type") but decompaction of the overburden was included in backstripping. Restoration scenario 3 used flexural balancing in order to account for the cohesive strength of the overburden, and included decompaction. Every restoration step used the respective average overburden thickness calculated during the preceding workstep to define an individual effective elastic thickness (Te) above salt. In all three scenarios the Zechstein evaporites and any surface and unit below were excluded from the unloading procedure.

Table 1: Stratigraphy and average rock properties used for backstripping and decompaction.

Lithostratigraphic Unit	Average Rock Type	Initial Porosity (%)	Depth Coefficient (km^{-1})	Density g/cm^3	Young Modulus (MPa)	Poisson Ratio
Upper North Sea Group	Sandstone	0.49	0.27	2.65	15000	0.29
Middle and Lower North Sea Group	Sandstone	0.49	0.27	2.65	15000	0.29
Chalk Group	Chalk	0.70	0.71	2.2	5810	0.4
Rijnland Group	ShalySand	0.56	0.39	2.68	23750	0.3
Schieland, Scruff and Niedersachsen Groups	ShalySand	0.56	0.39	2.68	23750	0.3
Altena Group	Shale	0.63	0.51	2.72	32500	0.3
Germanic Trias Group	Shale	0.63	0.51	2.72	32500	0.3
Zechstein Group	Shale	unbalanced	unbalanced	2.2	unbalanced	unbalanced

After every unloading step, the evaporite volume below the backstripped top Zechstein surface was readjusted and

105   restored to the initial model volume (ca. 6.38 x 10^{12} m³) by shifting the base Zechstein surface upwards. The geometry (form)

of the Zechstein base and the Zechstein volume were kept constant in all reconstruction steps. Unloading thus only caused

surface change down to top Zechstein, which, when plotted against the (solely in height) adjusted but geometrically constant

base Zechstein, enabled the calculation of a series of differential 3D salt thickness maps (Fig. 4). Resulting incremental changes

in Zechstein thickness were then plotted as loss-gain (Fig. 5) and salt movement maps (Fig. 6).

110   Identical restoration results could have been achieved by moving the top Zechstein and overburden downwards to

keep the salt volume constant. The restoration methodology proposed is thus independent of a reference datum, but

consequently does not support surface-topography or palaeo-geographic reconstruction. The restoration approach is limited to

incrementally backstrip the shallow post-salt overburden for the sole purpose of 3D true-to-volume reconstruction of the salt

substratum, explicity excluding balancing of the isostatic crust-mantle relationship. The method therefore cannot be compared

115   with classic crustal backstripping of salt systems (sensu Rowan, 2003; basic principles in Turcotte and Schubert, 2014).

3 Salt thickness reconstruction and salt loss-gain plots

True-to-volume Zechstein unloading in six time steps of ca. 25 - 50 Myrs duration restored the 3D subsurface

evaporite thickness and distribution between today and 251 Ma (Fig. 4). Key differences between the three example scenarios

120   are the omission (Fig. 4A) versus the inclusion of overburden decompaction during backstripping (Figs. 4b, c); and the use of

pure vertical unloading ("Airy unloading"; Figs. 4a and b) versus flexural overburden balancing (Fig. 4c). At first sight,

Zechstein isopachs between today and 200 Ma appear in all reconstructions relatively similar. A significant difference

characterizes all three restoration scenarios in the interval between 200 and 251 Ma. At 251 Ma, all reconstructions restore

major Zechstein thickness maxima (>1.5 km) in the Lower Saxony Basin (LSB) and in the northern Lauwerszee Trough (LT),

125   irrespective of the reconstruction approach used (Fig. 4). Few isolated thickness maxima remain more or less fixed at all times

in restoration scenarios 1 and 2 that apply pure vertical unloading (Figs. 4a, b). These maxima correspond to piercement salt

diapirs (e.g. Pieterburen, Winschoten) that remain unbalanced due to the lack of a vertical overburden. Such unbalanced salt
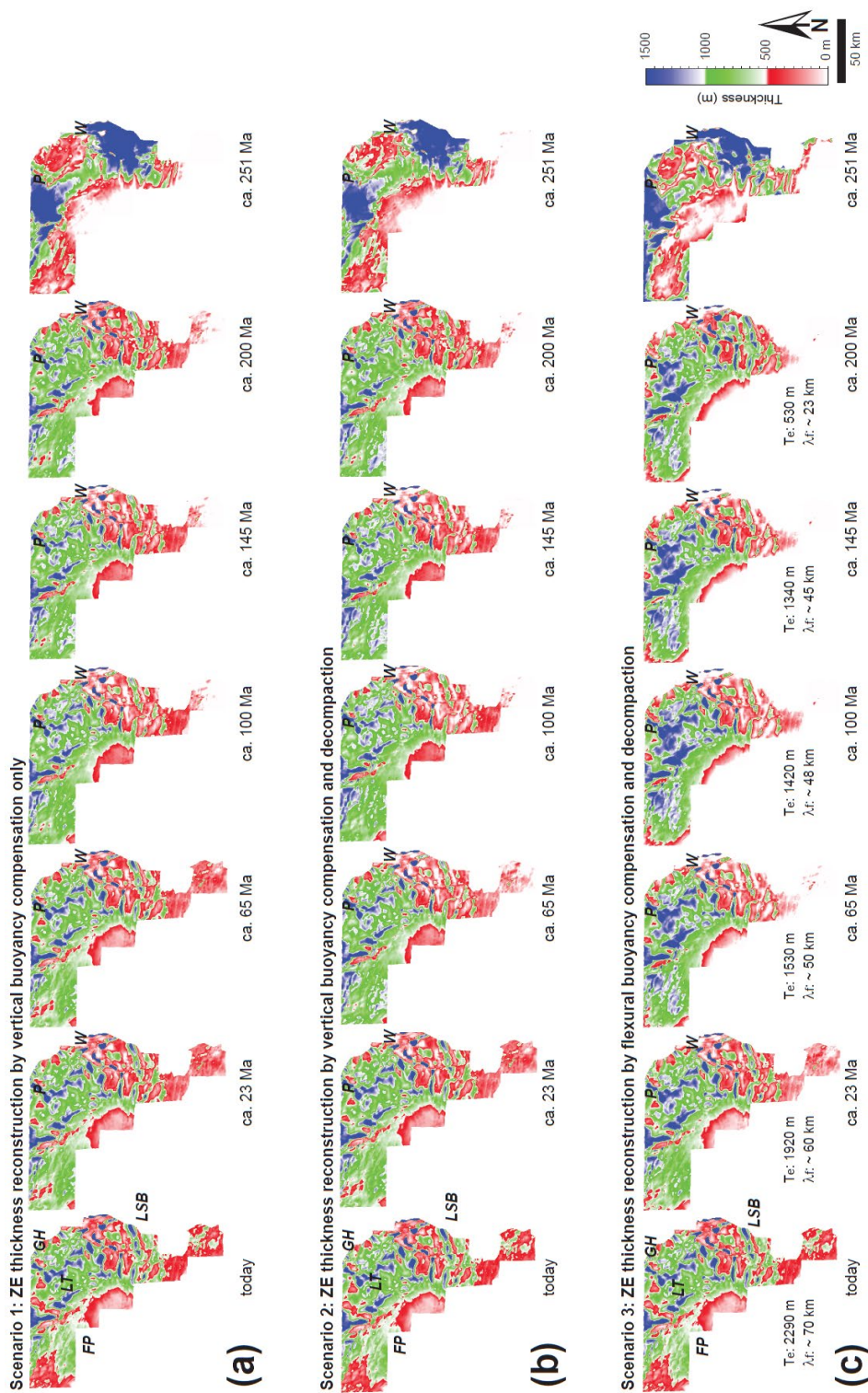
Figure 4. 3D Zechstein thickness-reconstruction results by backstripping. Note 251 Ma thickness maximum of Zechstein in Lower Saxony Basin (LSB) and Lauwerszee Trough (LT) in all reconstructions. (a) Backstripping scenario 1 – restored Zechstein thicknesses by vertical buoyancy compensation ("Airy balancing") omitting decompaction. (b) Backstripping scenario 2 - restored Zechstein thicknesses by vertical buoyancy compensation ("Airy balancing") including decompaction. (c) Backstripping scenario 3 - restored Zechstein thicknesses by flexural buoyancy compensation including decompaction. Effective elastic thickness (Te) of the overburden calculated as average overburden thickness from preceding restoration step; note corresponding change of flexural wavelength (λ_f) during backstripping. FP = Friesland Platform; GH = Groningen High; P = Pieterburen; W = Winschoten.
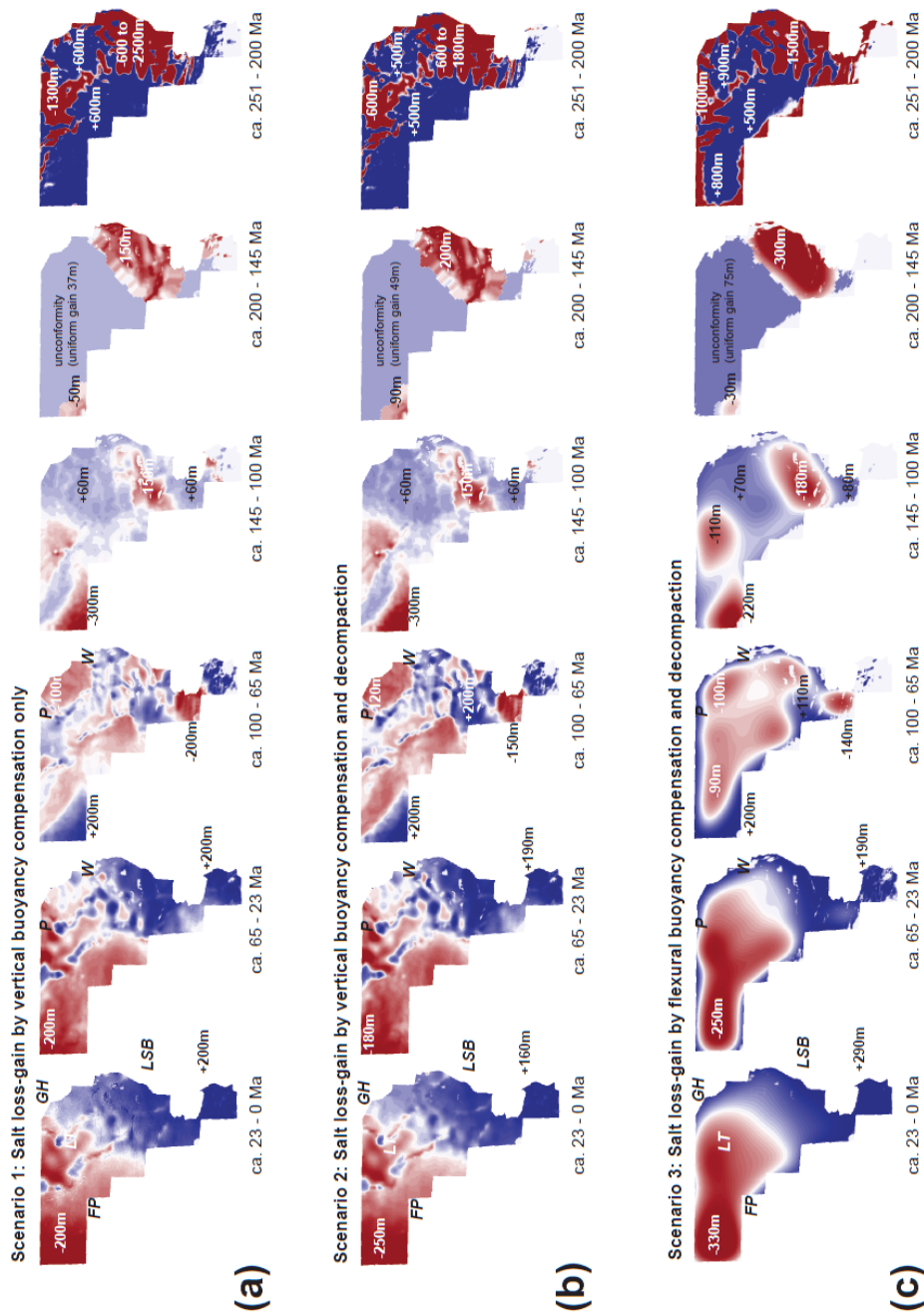
Figure 5: Differences calculated between successive pairs of isopachs of Figure 4. (a) Salt loss-gain plot of backstripping scenario 1. (b) Salt loss-gain plot of backstripping scenario 2. (c) Salt loss-gain plot of backstripping scenario 3. Note similarity between vertical buoyancy compensation of backstripping scenarios 1 and 2 documenting limited significance of decompaction. Note pronounced difference between flexural buoyancy compensation (c) and vertical balancing (a, b) between recent time and the Early Cretaceous (145-100 Ma).
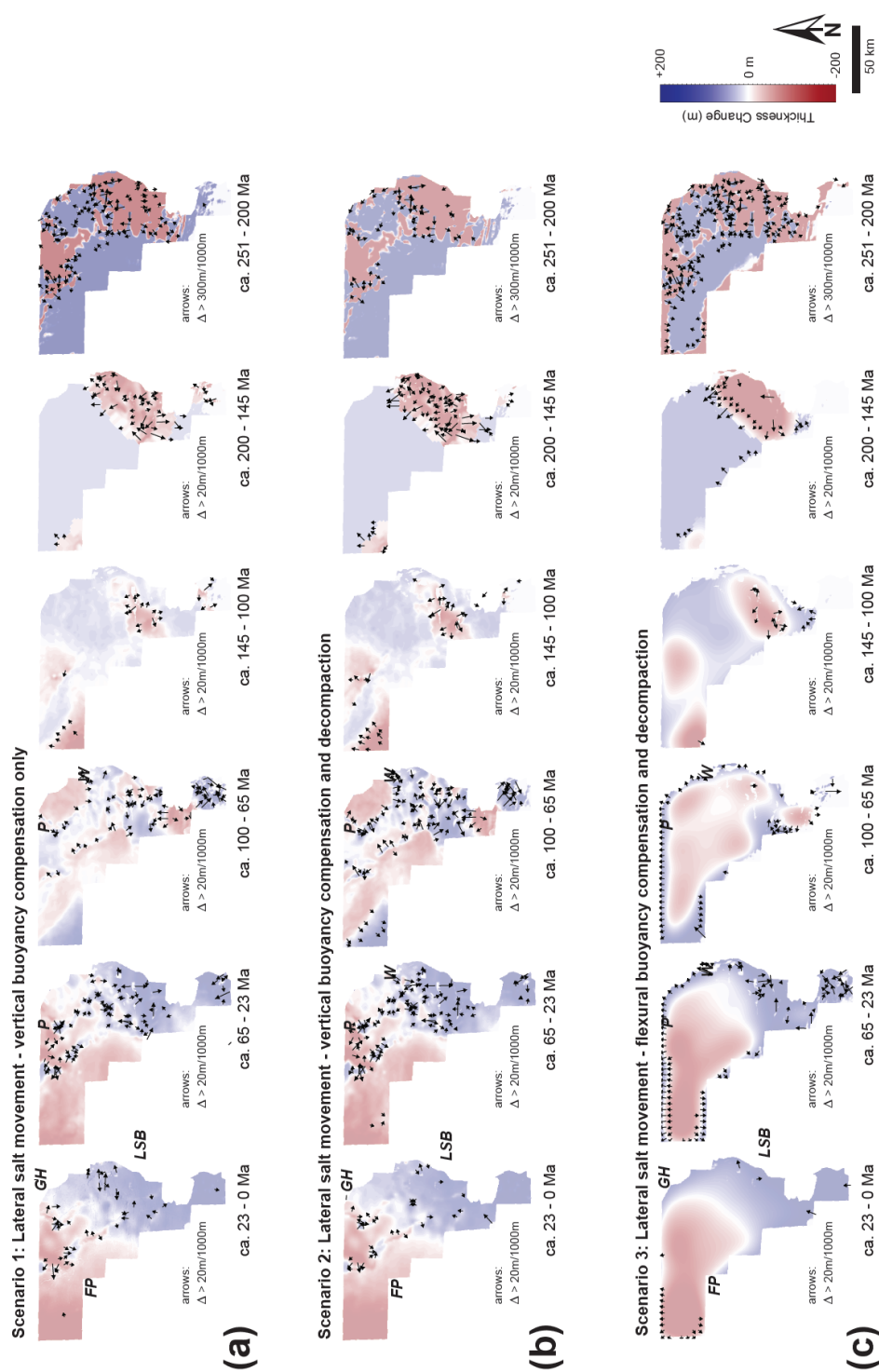
Figure 6: Maximum lateral change derived from difference plots of Figure 5. (a) Orientation of maximum lateral change based on backstripping scenario 1. (b) Orientation of maximum lateral change based on backstripping scenario. (c) Orientation of maximum lateral change based on backstripping scenario 3. Note pronounced edge effects at northern boundary of study area associated with flexural backstripping (scenario 3).

structures account for less than 5% of the total Zechstein model volume in scenarios 1 and 2 (Figs. 4a, b). In restoration

130   3, salt piercement structures change their shape during reconstruction due to overburden flexure affecting neighbouring areas.

In contrast to the rather subtle differences in Zechstein isopachs (Fig. 4), the difference plots between successive pairs

of isopach maps (Figs. 5 and 6) show considerable variation. Salt loss and gain of several hundreds of metres to >1 km are

highest in all restoration scenarios in the Triassic (251 - 200 Ma); at this time, major salt loss characterizes the LSB, less salt

loss the northern LT (Fig. 5). In all restoration scenarios salt escape is mainly to the Friesland Platform (FP) and Groningen

135   High (GH), both gaining between ca. 500 m (Scenario 2, Fig. 5b) and 900 m (Scenario 3, Fig. 5c) of evaporites. The Jurassic

(200-145 Ma) difference maps display uniform salt gain across most of the study area due to the presence of the Base

Cretaceous unconformity. The LSB shows in this time subsurface salt loss between 150 m (Scenario 1, Fig. 5a) and 300 m

(Scenario 3, Fig. 5c); the FP shows salt loss between 30 and 90 m (Fig. 5).

The Early Cretaceous (145-100 Ma) shows in all restorations only minor change in subsurface Zechstein distribution

140   (Figs. 5, 6). Main salt-loss areas are the northern LSB and the eastern FP (Fig. 6). Salt gain is mainly observed in the central

and southern LT and along the Hantum fault zone (Fig. 7). The Early Cretaceous (145-100 Ma; Fig. 5c) highlights the

difference between flexural backstripping and vertical overburden balancing (Figs. 5a, b) in producing a smoothed, partially

amplified salt loss and gain plot.

Between 100 and 65 Ma, the GH, LT and eastern FP are main expulsion areas, whereas the LSB and FP locally

145   receive >200 m of evaporites (Fig. 5). Vertical balancing with and without decompaction (Figs. 5b, c) documents the growth

of two narrow, parallel chains of NW-SE directed salt rollers, anticlines and walls above the main boundary faults of the LT

(Fig. 7). These structures receive more salt between 65 and 23 Ma (Figs. 6a, b). The LSB accretes in the Paleogene and

Neogene on average ca. 200 m of evaporites, respectively, likely sourced from the GH, LT, FP and from regions east (outside)

of the study area (Figs. 5, 6). Flexural balancing (Figs. 5c, 6c) does not provide sufficient lateral resolution for the determination

150   of Late Cretaceous to recent salt flow into individual salt structures.
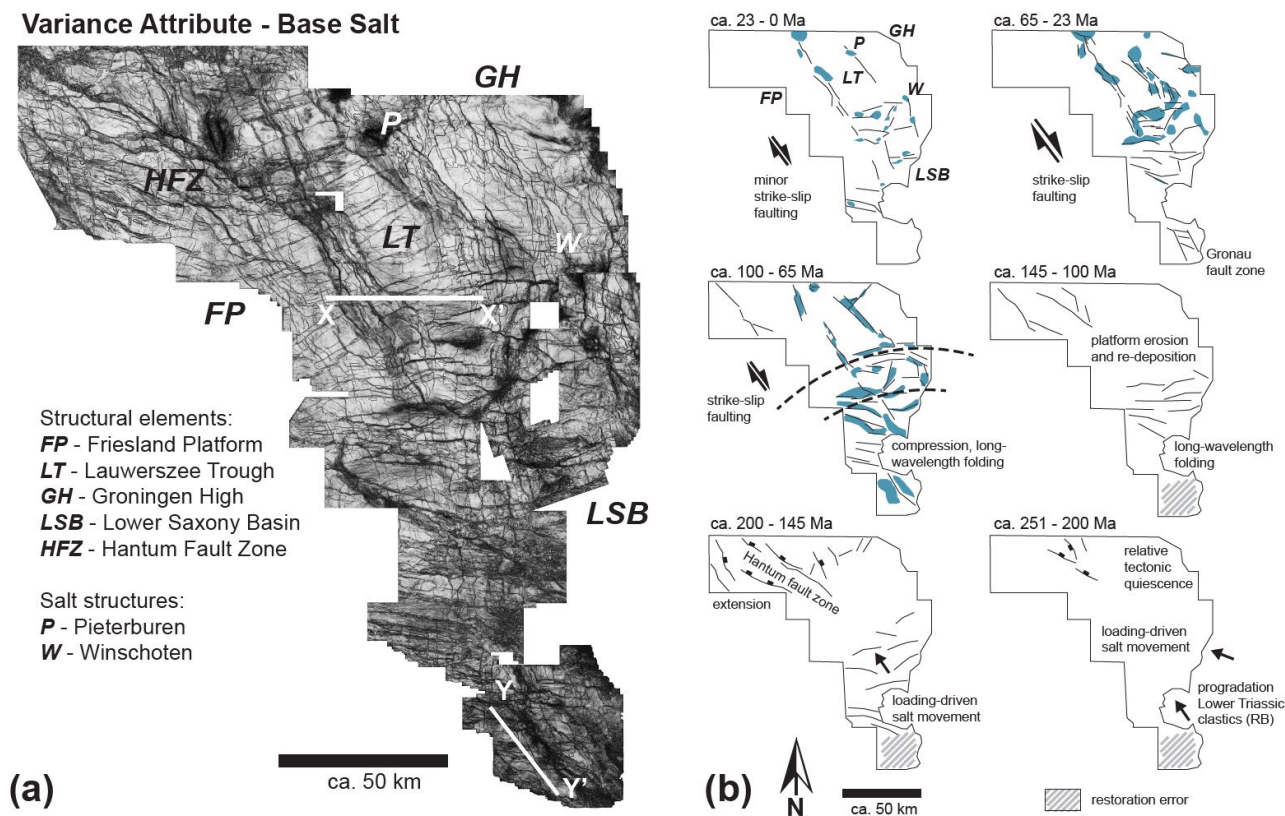
Figure 7. (a) 3D variance horizon-slice highlighting main structures of the pre-Zechstein. Hantum Fault Zone (HFZ) between FP and LT

155   characterized by significant salt gain in the Early Cretaceous. (b) Interpretation of relationship between sedimentary processes, tectonics and

subsurface salt movement. Lines X-X' and Y-Y' shown on Figure 3.

4 Geological interpretation

The Zechstein isopach maps (Fig. 4), the evaporite loss-gain calculations (Fig. 5), and the salt-movement plots (Fig.

160   6) provide important geological information when integrated with tectonic and seismic-stratigraphic analysis (Figs. 3a, b; 7;

also see Cartwright et al., 2001; Giles and Rowan, 2012; Alsop et al., 2016; Khalifa and Back, 2021). Salt loss can be

interpreted when top salt strata forms a thickened overburden. If subsurface evaporites are completely expelled, a salt weld

forms. Expulsion forces salt to move elsewhere, and salt either escapes to the surface and dissolves, or flows into salt structures

overlain by an isopach thin, if rising syn-depositionally. Other isopach anomalies, e.g. elongate minima or maxima above

165   basement-rooted structures (Figs. 3a, b; 4, 5, 7a) can indicate tectonically triggered subsurface salt loss or gain.

The thickness reconstructions of Figure 4 document that most parts of the study area were constantly underlain by

Zechstein evaporites. Exceptions are i) several large, mainly E-W-oriented salt welds in the northern LSB, and ii) the very

south of the study area with a complete lack of reconstructed Zechstein between 200 and 100 Ma (Fig. 4). The loss-gain plots

of the south indicate salt expulsion between 251 and 200 Ma; insignificant gain and loss until 100 Ma; and finally allochthonous

170   salt accretion since 65 Ma (Figs. 5, 6). The pre-65 Ma interpretation of the south must be, however treated with caution: lack

of much of the Mesozoic overburden due to erosion (Fig. 3a, b; 4) results in incomplete Top-Zechstein backstripping; the

restored Zechstein base therefore locally intersects the Zechstein top during unloading, producing significant restoration errors.

The locally restored 251 Ma salt thickness of the south (up to 200m) is yet similar to the salt-thickness reconstruction by Ten

Veen et al. (2012).

175   Evaporite-thickness change (Fig. 5) divided by the duration of each restoration interval documents that between 200

Ma and present-day, long-term Zechstein thickness change was up to ca. 15 m/Myr. Though low in rate, this change is

significant for interpretations on period or epoch scale (Fig. 5). For example, the ca. 150 m growth of salt ridges above the

eastern and western boundary faults of the LT in the Late Cretaceous can be interpreted as reflecting overburden thinning due

to inversion tectonics responding to Africa-Iberia-Europe convergence (sensu Kley and Voigt, 2008). The "Airy-type" salt-

180   movement plots between 100 and 23 Ma (Figs. 6a; b) all show significant salt flow above pre-existing, re-activated faults

(boundary faults LT; Figs. 3a, b; 7b) into salt diapirs and walls. However, this post-Triassic evaporite re-distribution is

generally small when compared to the isopach change between 251 and 200 Ma (Figs. 4, 5). The Triassic Zechstein re-

distribution is locally >1500 m (Fig. 5). Long-term evaporite loss (period scale) in the LSB and LT is at this time >30 m/Myr.

The Triassic evaporite expulsion can be interpreted as dominantly driven by sedimentary loading from the southeast during

185   the Buntsandstein (duration <10 Myrs; Figs. 2, 3, 4, 7B) in an overall tectonically quiet basin (Mohr et al., 2005; Geluk, 2007;

Vackiner et al. 2013; Strozyk et al., 2014). Thus, loading-driven salt flow might attain on epoch scale long-term rates of >150

m/Myr (in line with Zirngast, 1996; Kukla et al., 2008), which is significantly above the tectonics-driven long-term rate of up

to ca. 10 m/Myr in the Late Cretaceous (Fig. 5).

5 Discussion

190   3D application of the >2000-year-old principle of Archimedes (c. 246 BC) in the Zechstein salt system of the NE
Netherlands allows regional 3D thickness reconstruction of subsurface evaporites over time; 3D measurement of subsurface
salt loss and gain over time; 3D salt-flow reconstruction over time; and the estimation of long-term salt-flow rates. The
reconstruction of 3D subsurface salt movement is – although in this study solely dependent on the unloading of differential
195   overburden thicknesses – not restricted to monitoring sedimentary processes only. Any process that results in differential
overburden thickness (including tectonics) will be also be balanced, as exemplarily shown for Late Cretaceous and Paleogene
diapir growth likely triggered by inversion tectonics (Figs. 5, 6).

Zechstein-thickness restoration enables monitoring the growth and decay of salt structures and salt welds, results that
can be immediately applied in e.g. petroleum systems models or for constraing physical fluid-dynamic models. It must be
200   however noted that the studied Zechstein unit is internally heterogeneous (Fig. 2b), with both vertical and lateral facies
variations. More competent lithologies are interbedded with the mobile Zechstein halite units including anhydrite and
carbonate stringers (see strong intra-Zechstein reflector, Fig. 3a). Lithological heterogeneity gives rise to rheological
heterogeneity, which may have an impact on the associated buoyancy. It must be therefore acknowledged that the assumption
of all Zechstein units as a homogeneous fluid of constant density is a major simplification and thus a likely source of errors.

205   The salt loss-gain and movement plots (Figs. 5, 6) indicate that much of the internal structural complexity of evaporite
successions (for examples see Richter-Bernburg, 1980; Strozyk et al., 2012, 2014; Biehl et al., 2014) can be explained by
recurrent changes between salt loss, salt gain and evaporite-flow direction through time. Spatial evaporite redistribution
through time seems both caused by but also causing highly variable intra-Zechstein stress conditions leading to complex
polyphase and polydirectional 3D evaporite deformation (e.g. Fig. 3a).

210   Approximation of top Zechstein as horizontal surface at sea level after final unloading (situation at 251 Ma, all
scenarios of Fig. 4) constrains the 251 Ma palaeo-depth of base Zechstein based on overburden unloading only. In other words,
the assumption of top Zechstein as having formed at base level approximates the palaeo-depth location of base Zechstein by
subtracting the restored 251 Ma Zechstein thickness from present-day sea level. It must be noted that the validity of this
approximation stands and falls with the validity of the zero-topography assumption for top Zechstein, as the salt restoration

215 method presented is not tied to any topographic reference level. Topographic referencing, potentially providing an alternative

quality control for the differential salt thickness calculation, could be achieved by integrating crustal isostatic balancing above

the earth's mantle (Rowan, 2003; Turcotte and Schubert, 2014) contemporaneously to salt-redistribution modelling into the

restoration process. We have not yet found a technical solution for such an integration; crustal isostatic balancing remains

therefore excluded from this balancing study.

220   Key limitations of the Zechstein reconstruction presented are the incomplete restoration due to overburden

unconformities; omission of subsalt deformation from restoration; lack of knowledge on loss of salt at piercement structures;

and potential loss or influx of salt at the edges of the study area. Incomplete salt restoration due to overburden erosion primarily

affects the south (Figs. 4; 7b); incomplete restoration of salt diapirs and piercement structures various locations. Yet, any

backstripping naturally fails to balance missing rock record unless stratal gaps and hiati are filled. Integration of stratigraphic

225 forward modelling (e.g. Granjeon, 2014; Grohmann et al., 2021) with backstripping might help closing some unconformable

gaps in the sedimentary record.

The salt reconstruction presented has furthermore omitted the restoration of any subsalt post-Zechstein deformation.

Yet, if type, timing and magnitude of subsalt faulting or folding can be determined, 3D fault reconstruction or unfolding can

be readily integrated into the restoration methodology proposed, in this case after unloading prior to true-to-volume base

230 Zechstein adjustment.

The magnitude of potential loss or influx of salt at the edges of the study area was finally estimated by comparing a

first-pass scenario 1 restoration solely based on 3D block Groningen (Fig. 2) with the scenario 1 restoration of the entire NE

Netherlands (Fig. 4a). This comparison showed before 200 Ma a mismatch between the regional and local scenario 1

reconstructions in the Groningen area of <10%. At 200 Ma, the large-scale restoration trailed the local Groningen balance by

235 0,14 x 10^{12} m³ (ca. 12% of block volume). At 251 Ma, the large-scale reconstruction showed a lack of Zechstein by 0,47 x

10^{12} m³ (ca. 40% of block volume) in the Groningen block in comparison to the local model. This imbalance between local

and regional reconstructions indicates that true-to-volume balancing highly depends on model size and the amount of

differential unloading. Highest precision true-to-volume balancing by unloading will be achieved in restorations that cover subsurface salt systems in full 3D extent; and in these systems in the youngest backstripping intervals.

240   The case study presented here for the onshore NE Netherlands concentrates on a structurally relatively simple area dominated by vertical subsidence, with little influence from thick-skinned tectonic activity. The applied method therefore yields in this area promising results. This may not work as successfully in other, more complex salt-tectonic provinces. For example, if applied to areas where allochthonous salt sheets flow at the surface (e.g. Gulf of Mexico: e.g. Fletcher et al., 1996; Fort and Brun, 2012); where complex structures such as salt canopies occur (e.g. Santos Basin: Jackson et al., 2015; Moroccan

245   margin: Neumaier et al., 2016); or where large salt nappes have flowed many 10's of kilometres seaward, accommodating long-distance lateral translation of the overburden relative to the base-salt (e.g. offshore Angola; Fort et al., 2004; Hudec and Jackson, 2004), the method applied here may prove insufficient. In such cases a reconstruction coupling 3D salt-thickness restoration and 3D tectonic retro-deformation might be successful.

6 Conclusions

250   1. 3D backstripping based on the ancient Archimedes' principle restored through time variations in 3D subsurface evaporite thickness; 3D salt loss and gain; 3D subsurface salt movement; and long-term salt-flow rates.

2. Sequential unloading of a solid sedimentary overburden floating on a pseudo-fluid evaporite substratum showed that subsurface evaporite movement reacts to any process that influences overburden thickness, in this case sedimentation, erosion and tectonics.

255   3. Limits of buoyancy-based 3D salt reconstruction include incomplete restoration due to overburden unconformities; uncertainty of the volumetric model integrity because of potential salt loss by dissolution; exclusion of subsalt deformation from restoration; and potential loss or influx of salt at the edges of the model area.

4. 3D subsurface salt restoration based on Archimedes' principle is mathematically simple and computationally quick.

260   The approach presented can be potentially integrated into existing backstripping workflows. It can furthermore serve as a benchmark for physics-based numerical modelling of salt tectonics.

Data availability. Access to all seismic-reflection, borehole and geological surface data at www.nlog.nl (Dutch Oil and Gas

portal). Lithology data from DINOLoket public database.

265   **Author contributions.** SB and SA performed data analysis. SB and SA interpreted the data under discussion with VS and RL.

SB, SA, VS and RL wrote the final manuscript.

Acknowledgements. We thank the Netherlands Organisation for Applied Scientific Research (TNO) and the Nederlandse

Aardolie Maatschappij (NAM) for seismic, borehole and horizon data; Schlumberger for Petrel software; and Petroleum

Experts (Petex) for MOVE software. We acknowledge 3 anonymous reviews on an earlier version of this manuscript. SA is

270   funded by German Research Foundation (DFG) grant 403093957.

References

Aarhenius, S., and Lachmann, R.: Die physikalisch-chemischen Bedingungen der Bildung der Salzlagerstätten und ihre
     Anwendung auf geologische Probleme, Geologische Rundschau, 3, 139-157, 1912.

275   Airy, G.B.: On the Computations of the Effect of the Attraction of the Mountain Masses as Disturbing the Apparent
     Astronomical Latitude of Stations in Geodetic Surveys, Transactions of the Royal Society of London, 145, p. 101-
     104, 1855.

Alsop, G.I., Weinberger, R., Levi, T., and Marco, S.: Cycles of passive versus active diapirism recorded along an exposed salt
     wall, Journal of Structural Geology, 84, p. 47-67, 2016.

280   Archimedes: On floating bodies, in: The Works of Archimedes - Edited in Modern Notation with Introductory Chapters, edited
     by: Heath, T.L., Cambridge Library Collection - Mathematics, p. 253-262, 246 BC/2009.

Barton, D.C.: Mechanics of formation of salt domes with special reference to Gulf coast salt domes of Texas and Louisiana.
     AAPG Bulletin, 17, p. 1025–1083, 1933.

Biehl, B., Reuning, L., Strozyk, F., and Kukla, P.: Origin and deformation of intra-salt sulphate layers: an example from the
285   Dutch Zechstein (Late Permian), International Journal of Earth Sciences, 103, p. 697-712, 2014.

Cartwright, J., Steward, S., and Clark, J.: Salt dissolution and salt-related deformation of the Forth Approaches Basin, UK
     North Sea, Marine and Petroleum Geology, 18, p. 757-778, 2001.

Casas, E., and Lowenstein, T. K.: Diagenesis of saline pan halite; comparison of petrographic features of modern, Quaternary and Permian halites, Journal of Sedimentary Petrology, 59, p. 724–739, 1989.

290   Davison, I.: Faulting and fluid flow through salt, Journal of the Geological Society, London, 166, p. 205–216, 2009.

Davison, I., Alsop, G. I., and Blundell, D. J.: Salt tectonics: some aspects of deformation mechanics, in: Salt Tectonics, edited by: Alsop, G. I., Blundell, D. J., and Davison, I., Geological Society, London, Special Publication 100, p. 1–10, 1996.

Duin, E.J.T, Doornenbal, J.C., Rijkers, R.H.B., Verbeek, J.W., and Wong, T.: Subsurface structure of the Netherlands: Results of recent onshore and offshore mapping, Netherlands Journal of Geosciences - Geologie en Mijnbouw, 85, p. 245 –

295   276, 2006.

Fletcher, R.C., Hudec, M., and Watson, I.A.: Salt glacier and composite sediment-salt glacier models for the emplacement and early burial of allochthonous salt sheets, in: Salt tectonics: a global perspective, edited by: Jackson, M.P.A., Roberts, D.G., and Snelson, S., American Association of Petroleum Geologists Memoir 65, p. 77-108, 1996.

Fort, X., Brun, J.-P., and Chauvel, F.: Salt tectonics on the Angolan margin, synsedimentary deformation processes, American

300   Association of Petroleum Geologists Bulletin, 88, p. 1523–1544, 2004.

Fort, X., and Brun, J.-P.: Kinematics of regional salt flow in the northern Gulf of Mexico, in: Salt Tectonics, Sediments and Prospectivity, edited by: Alsop, G.I., Archer, S.G., Hartley, A. J., Grant, N.T., and Hodgkinson, R., Geological Society of London, Special Publication 363, p. 265-287, 2012.

Geluk, M.C.: Permian, in: Wong, T.E., Batjes, D.A.J., and De Jager, J., eds., Geology of the Netherlands, Royal Netherlands

305   Academy of Arts and Sciences, Amsterdam, p. 63-84, 2007.

Gemmer, L., Ings, S.J., Medvedev, S., and Beaumont, C.: Salt tectonics driven by differential sediment loading: stability analysis and finite element experiments, Basin Research, 16, p. 199–218, 2004.

Giles, K.A., and Rowan, M.G.: Concepts in halokinetic-sequence deformation and stratigraphy, in: Salt Tectonics, Sediments and Prospectivity, edited by: Alsop, G.I., Archer, S.G., Hartley, A. J., Grant, N.T., and Hodgkinson, R., Geological

310   Society of London, Special Publication 363, p. 7-31, 2012.

Granjeon, D.: 3D forward modelling of the impact of sediment transport and base level cycles on continental margins and incised valleys, in: From Depositional Systems to Sedimentary Successions on the Norwegian Continental Margin,

edited by: Martinius, A.W., Ravnås, R., Howell, J. A., Steel, R. J., and Wonham, J. P., International Association of Sedimentologists Special Publication 46, p. 453-472, 2014.

315 Grohmann, S., Fietz, W.S., Nader, F.H., Romero-Sarmiento, M.-F., Baudin, F., and Littke, R.: Characterization of Late Cretaceous to Miocene source rocks in the Eastern Mediterranean Sea: An integrated numerical approach of stratigraphic forward modelling and petroleum system, Basin Research, 33, p. 846-874, 2021

Hudec, M., and Jackson, M.P.A.: Regional restoration across the Kwanza Basin, Angola: Salt tectonics triggered by repeated uplift of a metastable passive margin, American Association of Petroleum Geologists Bulletin, 88, p. 071-990, 2004.

320 Hudec, M., and Jackson, M.P.A.: Terra Infirma: understanding Salt Tectonics, Earth-Science Reviews, 82, p. 1-28, 2007.

Jackson, C.A.L., Jackson, M.P.A., Hudec, M.R., and Rodriguez, C.R.: Enigmatic structures within salt walls of the Santos Basin - Part 1: Geometry and kinematics from 3D seismic reflection and well data, Journal of Structural Geology, 75, p. 135-162, 2015.

Jackson, M.P.A., and Hudec, M.: Salt Tectonics: Principles and Practice, Cambridge University Press, 498 p., 2017.

325 Jackson, M.P.A., and Vendeville, B.C.: Regional extension as a geologic trigger for diapirism, Geological Society of America Bulletin, 106, p. 57-73, 1994.

Kehle, R.O.: Identifying suitable "piercement" salt domes for nuclear waste storage sites, Report PNL-2864 UC-70 prepared for the Office of Nuclear Waste Isolation under its Contract with the U.S. Department of Energy, Batelle Memorial Institute, p. 1-30, 1980.

330 Kehle, R.O.: The origin of salt structures, in B.C. Schreiber, ed., Evaporites and Hydrocarbons, Columbia University Press, New York, p. 345-404, 1988.

Khalifa, N., and Back, S.: Folding and faulting offshore Libya: Partly decoupled tectonics above evaporites, Marine and Petroleum Geology, 124, 104840, 2021.

Kley, J., and Voigt, T.: Late Cretaceous intraplate thrusting in central Europe: Effect of Africa-Iberia-Europe convergence, not Alpine collision, Geology, 36, p. 839-842, 2008.

335 Koyi, H.A.: Modeling the influence of sinking anhydrite blocks on salt diapirs targeted for hazardous waste disposal, Geology, 29, p. 387-390, 2001.

Kukla, P.A., Urai, J.L., Mohr, M.: Dynamics of salt structures, in: Dynamics of complex intracontinental basins: The Central European Basin System, edited by Littke, R., Bayer, U., Gajewski, D., and Nelskamp, S., Berlin, Springer-Verlag, p. 291-306, 2008.

Mohr, M., Kukla, P.A., Urai, J.L., and Bresser, G.: Multiphase salt tectonic evolution in NW Germany: seismic interpretation and retrodeformation, International Journal of Earth Sciences, 94, p. 917-941, 2005.

Morley, C.K., and Guerin, G.: Comparison of gravity-driven deformation styles and behaviour associated with mobile shales and salt, Tectonics, 15, p. 1154-1170, 1996.

Nettleton, L.L.: Recent experiments and geophysical evidence of mechanics of salt dome formation, AAPG Bulletin, 27, p. 51-63, 1934.

Neumaier, M., Back, S., Littke, R., Kukla, P.A., Schnabel, M., and Reichert, C.: Late Cretaceous to Cenozoic geodynamic evolution of the Atlantic margin offshore Essaouira (Morocco), Basin Research, 28, p. 712-730, 2016.

Richter-Bernburg, G.: Salt Tectonics, Interior Structures of Salt Bodies, Bulletin Centres Recherches Exploration-Production Elf Aquitaine, 4, p. 373-389, 1980.

Rowan, M.G.: A systematic technique for the sequential restoration of salt structures, Tectonophysics, 228, p. 331-348, 2003.

Sclater, J.G., and Christie, P.A.F.: Continental stretching: An explanation of the Post-Mid-Cretaceous subsidence of the central North Sea Basin, Journal of Geophysical Research, 85, p. 3711-3739, 1980.

Strozyk, F., van Gent, H.W., Urai, J.L., and Kukla, P.A.: 3D seismic study of complex intra-salt deformation: An example from the Upper Permian Zechstein 3 stringer, western Dutch offshore, in: Salt Tectonics, Sediments and Prospectivity, edited by: Alsop, G.I., Archer, S.G., Hartley, A.J., Grant, N.T., and Hodgkinson, R., Geological Society, London, Special Publication 363, p. 489-501, 2012.

Strozyk, F., Urai, J.L., van Gent, H.W., de Keijzer, M., and Kukla, P.A.: Regional variations in the structure of the Permian Zechstein 3 intrasalt stringer in the northern Netherlands: 3D seismic interpretation and implications for salt tectonic evolution, Interpretation, 2, p. SM101-SM117, 2014.

Ten Veen, J.H., van Gessel, S.F., and den Dulk, M.: Thin- and thick-skinned salt tectonics in the Netherlands; a quantitative approach, Netherlands Journal of Geosciences - Geologie en Mijnbouw, 91, p. 447-464, 2012.

TNO-NITG: Geological Atlas of the Subsurface of the Netherlands – onshore, Netherlands Organisation for Applied Scientific Research, 103 p., 2004.

365   Trusheim, F.: Über Halokinese und ihre Bedeutung für die strukturelle Entwicklung Norddeutschlands, Zeitschrift der deutschen geologischen Gesellschaft (ZDGG), 109, p. 111–151, 1957.

Trusheim, F.: Mechanism of salt migration in northern Germany, AAPG Bulletin, 44, p. 1519–1540, 1960.

Turcotte, D., and Schubert, G.: Geodynamics, Cambridge University Press, 636 p., 2014

Vackiner, A.A., Antrett, P. Strozyk, F., Back, S., Kukla, P.A., and Stollhofen, H.: Salt kinematics and regional tectonics across
370   a Permian gas field: a case study from East Frisia, NW Germany, International Journal of Earth Sciences, 102, p. 1701-1716, 2013.

Van Adrichem Boogaert, H.A. & Kouwe, W.F.P.: Stratigraphic nomenclature of the Netherlands, revision and update by RGD and NOGEPA, Section A, General, Mededelingen Rijks Geologische Dienst 50: 1-40, 1993.

Van Dalfsen, W., Doornenbal, J.C., Dortland, S., and Gunnink, J.: A comprehensive seismic velocity model for the Netherlands
375   based on lithostratigraphic layers, Netherlands Journal of Geosciences - Geologie en Mijnbouw, 85, p. 277 – 292, 2006.

van Keken, P.E., Spiers, C.J., van den Berg, A.P., and Muyzent, E.J.: The effective viscosity of rocksalt: implementation of steady-state creep laws in numerical models of salt diapirism, Tectonophysics, 225, p. 457–476, 1993.

Waltham, D.: Why does salt start to move?, Tectonophysics, 282, p. 117-128, 1997.

380   Warren, J.K.: Evaporites, Springer International Publishing, 1813 p., 2016.

Wong, T.E., Batjes, D.A.J., and de Jager, J. (Eds.): Geology of the Netherlands, Amsterdam, Royal Netherlands Academy of Arts and Sciences (KNAW), 354 p., 2007.

Zirngast, M.: The development of the Gorleben salt dome (northwest Germany) based on quantitative analysis of peripheral sinks, in: Salt Tectonics, edited by: Alsop, G.I., Blundell, D.J., and Davison, I., Geological Society, London, Special
385   Publication 100, p. 203-226, 1996.